

# Aligned silver nanorod arrays produce high sensitivity surface-enhanced Raman spectroscopy substrates

Stephen B. Chaney<sup>a)</sup>

*Department of Physics and Astronomy, and Nanoscale Science and Engineering Center, University of Georgia, Athens, Georgia 30602*

Saratchandra Shanmukh and Richard A. Dluhy

*Department of Chemistry and Nanoscale Science and Engineering Center, University of Georgia, Athens, Georgia 30602*

Y.-P. Zhao

*Department of Physics and Astronomy, and Nanoscale Science and Engineering Center, University of Georgia, Athens, Georgia 30602*

(Received 7 March 2005; accepted 25 May 2005; published online 13 July 2005)

Substrates consisting of silver nanorod arrays with an irregular surface lattice (i.e., random nucleation sites) and with varying rod lengths were fabricated by an oblique angle vapor deposition method. These arrays were evaluated as potential surface-enhanced Raman spectroscopy (SERS) substrates using trans-1,2-bis(4-pyridyl)ethene as a reported molecule. SERS activity was shown to depend upon the length of the nanorods. The Ag nanorods with average lengths of  $508.29 \pm 44.86$  nm, and having aspect ratios of  $5.69 \pm 1.49$  exhibited the maximum SERS enhancement factors of greater than  $10^8$ . Theoretical calculations indicate that this large SERS enhancement may be partially explained by the shape, density, and lateral arrangement of the Ag nanorod arrays. © 2005 American Institute of Physics. [DOI: 10.1063/1.1988980]

Surface-enhanced Raman scattering (SERS) has emerged as a routine and powerful tool for the investigation and structural characterization of interfacial and thin-film systems.<sup>1-3</sup> In spite of its recent popularity, SERS does have limitations, including strict requirements that must be met in order to achieve optimal enhancement. One of the critical aspects of the technique involves the need for producing an ideal surface morphology on the SERS substrate for maximum enhancement, a requirement that is predicted from long-range classical electromagnetic (EM) theory.<sup>4-6</sup> Experimentally, the challenge of achieving an ideal reproducible surface morphology on a metal surface can be quite daunting. This fundamental limitation demonstrates the need for fabrication methods that produce reproducible and practical SERS-active substrates.

In recent years, vapor-deposited Ag metal films and Ag nanoparticles have gained favor as SERS substrates.<sup>7-11</sup> Standard vapor deposition methods result in silver island films (AgIF) of discontinuous particles of ellipsoidal geometry that are more stable than metal sols and produce a surface of particles that are more uniform in shape than the electrochemical method. Unfortunately, SERS enhancements obtained from these substrates tend to be lower than those obtained from colloidal aggregates. However, the combination of vapor deposition with nanosphere or e-beam lithographic procedures produces regular arrays of Ag nanoparticles that exhibit large SERS intensities. In addition, the size, shape and spacings of these Ag nanostructures can be controlled to tune the optical properties of the nanoparticle arrays.<sup>11-13</sup>

Research with nanoparticles has shown that the size, shape, and structural arrangement of the nanofabricated metallic particles are extremely important variables in achieving maximum SERS enhancement. For example, Au nanorods

exhibited stronger SERS signals than Au nanoparticles,<sup>14</sup> and an optimal nanorod aspect ratio was needed to reach the maximum enhancement.<sup>15</sup> Specially aligned nanorods have been shown to exhibit large SERS enhancement factors.<sup>16</sup> Unfortunately, many of the previous methods reported for preparing metallic nanoparticle arrays for high sensitivity SERS applications are expensive or time consuming, and it is difficult to easily prepare reproducible metal-coated substrates of the correct surface morphology to provide maximum SERS enhancements.<sup>3</sup>

Based on these previous studies, it appears that two major factors are necessary in order to achieve high SERS enhancements using nanoparticle arrays: A high aspect ratio nanorod and an optimized spatial arrangement of the nanoarray. In principle, then, by carefully tuning the size, shape and

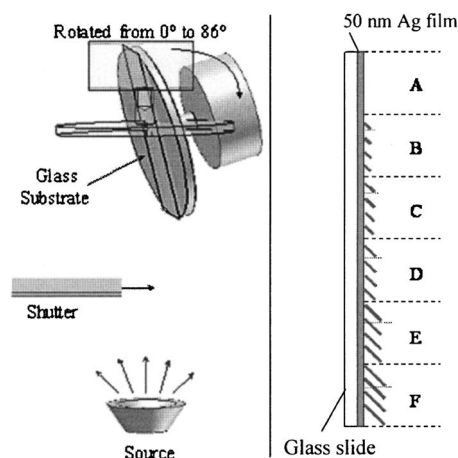


FIG. 1. (a) Experimental setup for OAD. A high-vacuum motor was used to rotate the substrate in the polar direction. A manual shutter was used to continue to block the incoming vapor so that six different regions with different nanorod lengths can be formed. (b) A schematic diagram showing the six regions after deposition.

<sup>a)</sup>Electronic mail: schaney@uga.edu

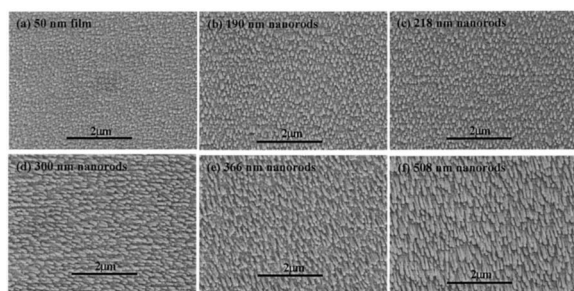


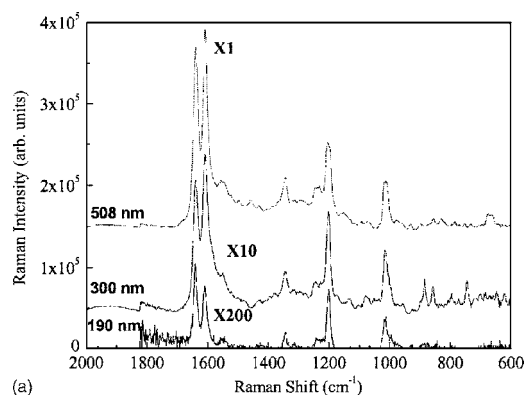
FIG. 2. SEM images of the six different regions with Ag nanorod lengths of (a)  $\ell=0$ , (b) 190, (c) 218, (d) 300, (e) 366, and (f) 508 nm, respectively. Since the SEM images for each individual region were obtained from smaller pieces cut from the original six-region substrate, the directions of the nanorods were not aligned during the measurement.

arrangement of these nanoparticle arrays, one may achieve a maximum enhanced EM field. We believe that a simple physical vapor deposition method, oblique angle vapor deposition, offers a flexible, easy, and inexpensive method for the fabrication of high aspect nanorod arrays for high sensitivity SERS applications.

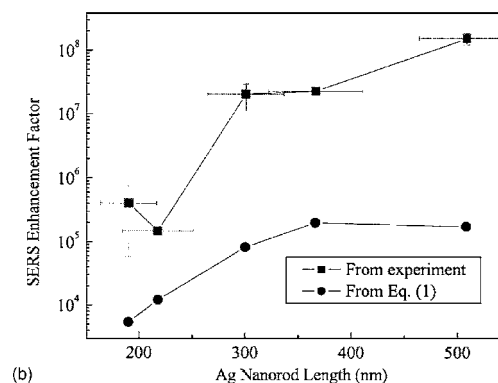
Oblique angle deposition (OAD) is a physical vapor deposition technique<sup>17</sup> in which the substrate is rotated in the polar direction by a stepper motor, as shown in Fig. 1. During deposition, the angle between the incoming vapor from the source and the surface normal of the substrate is set to be greater than  $75^\circ$ . The main mechanisms that control the growth are the shadowing effect and surface diffusion. OAD is simple to implement, and any thin-film physical vapor deposition system can be readily changed to an OAD system.

The Ag nanorod substrates used in this study were fabricated using a custom-designed electron-beam/sputtering evaporation (e-beam) system. The substrate used in these experiments was a glass microscope slide with a typical dimension of 3 in.  $\times$  1 in.; the microscope slide was cleaned using standard clean-1 before loading into the substrate holder. The motion of the substrate holder was controlled by two vacuum stepper motors, one rotating in the polar direction and one rotating in the azimuthal direction, as shown in Fig. 1. A custom-designed substrate shutter was used to selectively reveal increasing portions (predetermined) of the substrate during the deposition process, thereby forming a multiregion Ag nanorod sample with varying Ag rod lengths within a single deposition. These regions are denoted as A, B, C, D, E, and F in Fig. 1(b). Typically, a base layer of a 50 nm Ag thin film was initially deposited at normal incidence, i.e., the substrate was face down to the evaporation source as shown in Fig. 1(a). The substrate was then rotated to an incident angle of  $86^\circ$ , after which Ag nanorods were deposited in steps of  $\sim 200$  nm by partially opening the shutter after each deposition. During deposition, the Ag thickness was checked by a film thickness monitor at normal incidence. Actual nanorod length for each deposition region was determined using a LEO 982 field emission scanning electron microscope (SEM). The average surface roughness and nanorod thickness was evaluated from atomic force microscopy (AFM) images using a DI NanoScope 3100.

Figure 2 shows six representative SEM images on different parts of the sample. For the 50 nm thick initial Ag deposition, Ag nanoparticles exist on the surface [Fig. 2(a)]. With increasing deposition time, randomly distributed but aligned nanorod arrays are developed on the substrate Figs.



(a)



(b)

FIG. 3. (a) The representative SERS spectra of BPE adsorbed onto Ag nanorods of length 190 nm, 300 nm, and 508 nm, respectively. The spectra for the 190 nm and 300 nm arrays were enlarged by a factor of 200 and 10, respectively. (b) The SERS enhancement factor calculated as a function of the Ag nanorod length. Experimentally determined SERS SEF (■), and SERS SEF theoretically calculated from the spheroid approximation (●).

2(b)–2(f). The length of the nanorods increases monotonically as a function of deposition time, and the nanorods are tilted with respect to the normal to the substrate surface. Previous results have shown that the tilt angle for these nanorods is between  $50^\circ$ – $60^\circ$  with respect to the substrate normal. SEM images were used to determine that the six separate regions had nanorod lengths of  $\ell=0$ ,  $190 \pm 26$ ,  $218 \pm 34$ ,  $300 \pm 36$ ,  $366 \pm 44$ , and  $508 \pm 45$  nm, respectively. The diameter of the Ag nanorods was estimated from AFM measurements to be  $\sim 80$ – $90$  nm, while the density of the nanorods was approximately  $15$ – $25 \mu\text{m}^{-2}$ .

These Ag nanorod arrays have been evaluated as SERS. SERS spectra were acquired as a function of the length of the nanorod using a near-IR (NIR) confocal Raman microscope at an excitation wavelength of 785 nm. The spectrograph used was a Kaiser Optical Systems Holospec  $f/1.8$ -NIR equipped with a LN<sub>2</sub>-cooled charge coupled device camera. Laser illumination at 785 nm was supplied by a Coherent Radiation 899 Ti:Sapphire laser pumped by a Innova 300 Ar<sup>+</sup>-ion laser.

The molecular probe used in this study was trans-1,2-bis(4-pyridyl)ethene [(BPE) Aldrich, 99.9+ %]. BPE was chosen as the probe to calculate enhancement factors because of its high Raman scattering cross section and its ability to adsorb strongly and irreversibly to a Ag substrate.<sup>18</sup> BPE solutions were prepared by sequential dilution in HPLC grade methanol (Aldrich). The concentration of the BPE and the volume applied were calculated to produce a surface coverage of  $\sim 0.21$  monolayers to avoid self-quenching effects.<sup>19,20</sup> A BPE solution was applied to each of the SERS

substrates and allowed to dry before the acquisition of spectra. The  $1200\text{ cm}^{-1}$  peak of BPE was chosen for the quantification because of its relative insensitivity to molecular orientation on a Ag surface. SERS spectra were collected at multiple locations on the sample for  $\sim 10$  s each with  $\sim 20$  mW laser power at the microscope objective.

Representative SERS spectra of BPE on Ag nanorod arrays with rod lengths of 508 nm, 300 nm, and 190 nm are presented in Fig. 3(a). For comparison with the 508 nm spectrum, the spectra for the 190 nm and 300 nm rods have been enlarged by  $200\times$  and  $10\times$ , respectively. It is clear from Fig. 3(a) that the SERS intensity increases dramatically with nanorod length. The SERS surface enhancement factor (SEF) was calculated for BPE on the stepped Ag nanorod samples according to the equation  $\text{SEF} = (I_{\text{surf}}/N_{\text{surf}})/(I_{\text{bulk}}/N_{\text{bulk}})$ . In this expression,  $I_{\text{surf}}$  and  $I_{\text{bulk}}$  denote the integrated intensities for the  $1200\text{ cm}^{-1}$  band of the BPE adsorbed on the Ag surface and BPE in solution, respectively; whereas  $N_{\text{surf}}$  and  $N_{\text{bulk}}$  represent the corresponding number of BPE molecules excited by the laser beam.

Figure 3(b) illustrates the calculated SERS SEF plotted as a function of the length of the Ag nanorod. The SEF increased from almost zero for Region A ( $\ell=0$  nm), to over  $10^5$  for a very short Ag nanorod in Region B ( $\ell=190$  nm), and then increased another three orders of magnitude ( $10^8$ ) for a nanorod in Region F ( $\ell=508$  nm). The intense SERS enhancement factors observed on these Ag nanorods ( $10^8$ ) are orders of magnitude larger than those obtained from previously published methods of forming nanoparticle arrays by vapor deposition ( $\text{SEF} \sim 10^4$ ),<sup>15,21</sup> and compare favorably to the best SERS enhancements reported using substrates prepared by elaborate nanolithographic procedures ( $\text{SEF} \sim 10^8$ ).<sup>22</sup> The maximum average SERS SEF calculated for multiple locations on a single substrate was  $1.39 \times 10^8$  for a Ag nanorod array measured at 508 nm. The reproducibility of the SERS SEF and nanorod height measurements is given by the error bars in Fig. 3(b). Only a very few experiments, including near-field SERS measurements ( $\text{SEF} \sim 10^{13}$ ) (Ref. 23) and substrates with specifically engineered nm-scale “hot spots” ( $\text{SEF} \sim 10^{14}$ ),<sup>24,25</sup> have demonstrated larger SERS enhancements than the Ag nanorod substrates described here.

It is likely that the large SERS enhancement factors for these substrates are due mainly to an electromagnetic dipole effect accentuated by the high aspect ratio of the Ag nanorods.<sup>26</sup> If we treat the Ag nanorods as prolate spheroid particles, the electric field at the tip of the spheroid is enhanced by a factor of  $f(\omega)$  [ $E_{\text{out}} = f(\omega)E_0$ ] and the Raman enhancement factor will be approximately proportional to  $|f(\omega)|^4$ . Under the modified long wavelength approximation given in equation (3) by Wokaun *et al.*, and using the bulk dielectric constant of Ag at 785 nm,<sup>28</sup> the calculated Raman enhancement factor is shown in Fig. 3(b). Although the theoretical estimation of SEF as a function of nanorod length follows a trend similar to that of the experimental data, the estimated SEF is much lower than that obtained experimentally. This discrepancy increases with increasing nanorod length. When  $\ell < 300$  nm, the discrepancy is less than two orders of magnitude, while when  $\ell \geq 300$  nm, the discrepancy increases to over two orders of magnitude. The discrepancy between experimental and calculated SEF is consistent with the change in morphology of the Ag nanorods as seen in

Fig. 2. For  $\ell < 300$  nm, there is no lateral overlap of the nanorods on the surface, while for  $\ell \geq 300$  nm, lateral overlap exists between adjacent nanorods. Therefore, the enhanced electric field is not only determined by the aspect ratio of a single nanorod, but also the lateral arrangement of the nanorod arrays, i.e., the enhanced field also depends upon the radiation fields generated by nearest-neighbor nanorods, as has been previously demonstrated using nanoparticle arrays.<sup>29</sup>

In summary, we have created a Ag nanorod substrate that is fabricated utilizing a vapor deposition technique that is easily implemented in the laboratory. These substrates achieve SERS enhancement factors of approximately  $10^8$  for arrays of Ag rods having a length of 508 nm and a width of 80–90 nm. These substrates reproduce SERS spectra with no discernable hot spots and show potential as high sensitivity substrates for SERS-based measurements.

Two of the authors (S.B.C.) and (Y.P.Z.) thank the support from the National Science Foundation (No. ECS-0304340). Two other authors (S.S.) and (R.A.D.) are supported by the U.S. Public Health Service through National Institutes of Health Grant (No. EB001956).

<sup>1</sup>T. Vo-Dinh, *Trends Analyt. Chem.* **17**, 557 (1998).

<sup>2</sup>K. Kneipp, H. Kneipp, I. Itzkan, R. R. Dasari, and M. S. Feld, *J. Phys.: Condens. Matter* **14**, R597 (2002).

<sup>3</sup>Z. Q. Tian, B. Ren, and D. Y. Wu, *J. Phys. Chem. B* **106**, 9463 (2002).

<sup>4</sup>J. Gersten and A. Nitzan, in *Surface Enhanced Raman Scattering*, edited by R. K. Chang and T. E. Furtak (Plenum, New York, 1982), p. 89.

<sup>5</sup>H. Metiu and P. Das, *Annu. Rev. Phys. Chem.* **35**, 507 (1984).

<sup>6</sup>M. Moskovits, *Rev. Mod. Phys.* **57**, 783 (1985).

<sup>7</sup>V. L. Schlegel and T. M. Cotton, *Anal. Chem.* **63**, 241 (1991).

<sup>8</sup>R. P. Van Duyne, J. C. Hulteen, and D. A. Treichel, *J. Chem. Phys.* **99**, 2101 (1993).

<sup>9</sup>S. E. Roark and K. L. Rowlen, *Anal. Chem.* **66**, 261 (1994).

<sup>10</sup>D. J. Semin and K. L. Rowlen, *Anal. Chem.* **66**, 4324 (1994).

<sup>11</sup>T. R. Jensen, G. C. Schatz, and R. P. Van Duyne, *J. Phys. Chem. B* **103**, 2394 (1999).

<sup>12</sup>T. R. Jensen, M. D. Malinsky, C. L. Haynes, and R. P. Van Duyne, *J. Phys. Chem. B* **104**, 10549 (2000).

<sup>13</sup>N. Féliđj, J. Aubard, G. Levi, J. R. Krenn, M. Salerno, G. Schider, B. Lamprecht, A. Leitner, and F. R. Aussenegg, *Phys. Rev. B* **65**, 075419 (2002).

<sup>14</sup>B. Nikoobakht and M. A. El-Sayed, *J. Phys. Chem. A* **107**, 3372 (2003).

<sup>15</sup>B. Nikoobakht, J. Wang, and M. A. El-Sayed, *Chem. Phys. Lett.* **366**, 17 (2002).

<sup>16</sup>A. Tao, F. Kim, C. Hess, J. Goldberger, R. He, Y. Sun, Y. Xia, and P. Yang, *Nano Lett.* **3**, 1229 (2003).

<sup>17</sup>L. Abelmann and C. Lodder, *Thin Solid Films* **305**, 1 (1997).

<sup>18</sup>K. L. Norrod, L. M. Sudnik, D. Rousell, and K. L. Rowlen, *Appl. Spectrosc.* **51**, 994 (1997).

<sup>19</sup>E. J. Zeman, K. T. Carron, G. C. Schatz, and R. P. Van Duyne, *J. Chem. Phys.* **87**, 4189 (1987).

<sup>20</sup>W. H. Yang, J. Hulteen, G. C. Schatz, and R. P. Van Duyne, *J. Chem. Phys.* **104**, 4313 (1996).

<sup>21</sup>S. P. Mulvaney, L. He, M. J. Natan, and C. D. Keating, *J. Raman Spectrosc.* **34**, 163 (2003).

<sup>22</sup>M. Green and F. M. Liu, *J. Phys. Chem. B* **107**, 13015 (2003).

<sup>23</sup>R. M. Stöckle, V. Deckert, C. Fokas, D. Zeisel, and R. Zenobi, *Vib. Spectrosc.* **22**, 39 (2000).

<sup>24</sup>S. M. Nie and S. R. Emery, *Science* **275**, 1102 (1997).

<sup>25</sup>K. Kneipp, H. Kneipp, R. Manoharan, E. B. Hanlon, I. Itzkan, R. Dasari, and M. S. Feld, *Appl. Spectrosc.* **52**, 1493 (1998).

<sup>26</sup>D.-S. Wang and M. Kerker, *Phys. Rev. B* **24**, 1777 (1981).

<sup>27</sup>A. Wokaun, J. P. Gordon, and P. F. Liao, *Phys. Rev. Lett.* **48**, 957 (1982).

<sup>28</sup>P. B. Johnson and R. W. Christy, *Phys. Rev. B* **6**, 4370 (1972).

<sup>29</sup>L. L. Zhao, K. L. Kelly, and G. C. Schatz, *J. Phys. Chem. B* **107**, 7343 (2003).